Annals of Nuclear Energy 160 (2021) 108387

Contents lists available at ScienceDirect

Annals of Nuclear Energy

journal homepage: www.elsevier.com/locate/anucene

# Effectiveness of the ASVAD valve in a reactor vessel bottom leak scenario

Jordi Freixa [a,*], Arnaldo Laborda [b], Victor Martinez-Quiroga [a]

[a] *Department of Physics, Universitat Politècnica de Catalunya (UPC), Spain*
[b] *ASVAD INTL SL, Tarragona, Spain*

ARTICLE INFO

*Article history:*
Received 15 January 2021
Received in revised form 21 April 2021
Accepted 30 April 2021

*Keywords:*
PWR
Nitrogen
Accumulator
ASVAD
Non-condensable

ABSTRACT

Decay heat removal can be seriously degraded by the presence of non-condensable gases in the cooling circuits. Nitrogen gas may be pushed into the primary system after a full discharge of the accumulators. This may produce various adverse effects: the interruption of natural circulation, the limitation of the primary to secondary heat transfer during the reflux cooling and prevent the startup of the active injection by stabilization of the pressure above the injection set point. State-of-the-art system codes have proven to be capable to simulate non-condensable gas effects in accident situations. The ASVAD valve, has been designed to avoid the inflow of nitrogen into the primary system by means of passive concepts. This paper addresses the complications derived from the nitrogen and evaluates the ASVAD valve performance through the simulation of a vessel bottom leak experiment at the LSTF facility in Japan.


## 1. Introduction

The capacity to extract the decay heat generated in the core of a nuclear reactor after a shutdown is one of the most important aspects of the design of a pressurized water reactor (PWR). In addition to the safety systems specifically designed to guarantee the safe extraction of the decay heat, PWR rely on the extraction of heat through the steam generators by means of the condensation mechanism that can take place under certain conditions. The condensation of steam in the primary system is an extremely powerful heat transfer process and PWR designs take advantage of this effect to maintain the system cooled.

During LOCA accidents, where the primary mass inventory is continuously lost, heat can be effectively extracted through the so called reflux and condensation process. The steam is created in the core of the reactor and flows into the primary side of the steam generators (SG) where it condenses due to the colder temperatures in the secondary side. The condensation water flows back to the core contributing to the cooling of the reactor.

Condensation heat transfer can be diminished in the presence of non-condensable gases. In this case, the heat transfer coefficient can be reduced by almost one order of magnitude practically blocking heat transfer (DeVuono and Christensen, 1984).

Current PWR designs such as Westinghouse or Konvoi designs are equipped with an accumulator system which consists of a tank filled with subcooled borated water. The tank is pressurized with nitrogen to a pressure around 4.5 MPa.

When the primary pressure falls below the initial accumulator pressure, water is pushed by the pressurized nitrogen into the primary system increasing the mass inventory and cooling the reactor. Accumulators were specially designed to cope with a LOCA accident but intervene in a broad number of sequences that imply a loss of cooling inventory. This system has the advantage of being fully passive (category A) according to the categorization made by IAEA (2009). But on the other hand, the nitrogen may flow into the primary system once the water has been depleted. To avoid the gas intrusion, a valve is mounted in the connection line that allow the operators to isolate the accumulator. Operator procedures have been laid down to guide the operator to isolate the accumulator system once the coolant is deemed to have almost depleted. It is worth noticing though, that in general no level measurements are present in the accumulators and the actions of the operators are based on the primary pressure evolution, i.e. the accumulator is thought to be empty at a certain primary pressure. In addition, in design basis accidents (DBA), operator actions are not credited unless they lead to a more unfavourable condition and therefore the possibility that nitrogen enters the primary system needs to be taken into account. If no operator action is performed, nitrogen will enter the primary system as soon as the Accumulator empties.

In addition to the reduction of the heat transfer coefficient under reflux&condenser conditions, in the cases where two phase flow natural circulation is established as the main heat extraction mechanism, the presence of non-condensable gases may cause the cease of the circulation. The gas may accumulate forming slugs,

* Corresponding author.
*E-mail addresses:* jordi.freixa-terradas@upc.edu (J. Freixa), alaborda@asvad-nuclear.com (A. Laborda), victor.martinez-quiroga@upc.edu (V. Martinez-Quiroga).

https://doi.org/10.1016/j.anucene.2021.108387
0306-4549/

when circulating through the heat exchanger, heat transfer suddenly decreases and diminishes the circulation driving force. This leads to a sudden increase in primary pressure and the natural circulation may resume. This process may be repeated several times (D'Auria et al., 2017).

For all these reasons, a new valve —the ASVAD valve —has been designed with the objective to completely avoid this undesired nitrogen injection. The ASVAD valve is fully passive. The goal of the present paper is to identify the complications derived from the presence of nitrogen inside the reactor coolant system (RCS), and to evaluate how the ASVAD valve can improve the safety of current reactors. In order to fulfill this objective a former experiment carried out at the Large Scale Test Facility (LSTF) operated by the Japan Atomic Energy Agency (JAEA) will be used. The selected experiment is Test 6–2 from the OECD/NEA ROSA-1 project, a leak at the bottom of the reactor pressure vessel (RPV) with unavailability of the High Pressure Safety Injection (HPSI) and asymmetric secondary side depressurization. This experiment has been selected for the present publication because the nitrogen effects are clearly shown. In this experiment, the nitrogen from the accumulators entered the primary system. The intense degradation of heat transfer pushed up the primary pressure preventing the system to reach the Low Pressure Safety Injection (LPSI) setpoint. The experiment had to be interrupted reducing the power of the reactor to prevent damage of the heating rods that simulate the core.

The present paper will firstly assess the capabilities of the system code RELAP to simulate the system behaviour of a PWR under the presence of non-condensable gases by comparison to the experiment. Afterwards, the implications of the addition of the ASVAD valve in the reactor will be evaluated by performing sensitivities.

## 2. Background on the modelling of non-condensable transport

Non-condensable gas tends to mix well with steam and thus is carried with the steam flow. There are three main mechanisms for the non-condensable transport:

1. Entrainment of gas by flowing steam.
2. Gravity forces arising from density differences.
3. Diffusion driven by the concentration gradient.

The first process is the dominant and is usually the only one considered in system codes such as RELAP, TRACE or ATHLET. Due to the design of PWR reactors, steam tends to be flowing from the core, where it is generated, to the SG primary side where it condensates and creates a contraction in pressure. Nitrogen is therefore carried to the U-tubes in the primary side of the SG, steam condensates and flows back to the core due to gravity. However, nitrogen accumulates in the U-tubes where condensation is taking place. With its presence, the condensation process diminishes or may even cease altogether. The consequence is a rise in primary pressure which implies a rise in the break flow. In addition, the increase in pressure may delay, avoid or reduce the active safety systems such as the high and low pressure injection systems. Riikonen et al. (2018) provided a detailed description of the consequences of nitrogen inflow in different transient scenarios.

In addition to these adverse consequences, Steinbrück et al. (2017) provided evidence of the contribution of nitrogen to accelerate the oxidation of the zirconium cladding due to the presence of nitrogen, even at low concentrations. Other studies pointed out that when this gas reaches the pipes of the emergency systems, it disturbs their proper work causing cavitation, water hammer and pump voiding effects (US-NRC, 2008).

The effect of nitrogen inside the RCS system was studied in some experiments starting with the BETHSY experiments in 1994 (Noel and Derauz, 1994). The inflow of nitrogen into the primary system has been investigated in most of the experimental programs that study the evolution of accidental sequences for PWR reactors such as the OECD/NEA PKL program series (Umminger et al., 2012), the OECD/NEA ATLAS (Song et al., 2015) and the OECD/NEA ROSA 1 (NEA, 2013) and 2 (OECD/NEA, 2017) projects.

Other research programs have focused on separate effect testing on the influence of nitrogen on the heat transfer in the U-tubes of PWR reactors. Of particular interest are the works from Liu (2001), Lee et al. (2006a) and Woods et al. (2009).

State of the art of system codes have proven to be capable to cope with non-condensable gas effects in accident situations although with some limitations. Several authors have published simulations of experiments where non-condensable gases play a significant role: Mukin et al. (2018), Freixa et al. (2020), Freixa (2012), Takeda et al. (2016) and Gallardo et al. (2011). System codes have different approaches to represent the reduction of the heat transfer coefficient in the presence of non-condensable gases but in general most system codes use multiplication factors to the heat transfer coefficients for the steam/water mixture (Austregesilo et al., 2003; United States Nuclear Regulatory Commission, 2007). In RELAP5, the presence of a noncondensable gas is represented by the mass fraction ($X_n$) of the combination of noncondensable and steam which is attributable to the noncondensable gas (Information Systems Laboratories, 2010). The effects of a noncondensable gas are represented by multipliers that modify and reduce the volumetric heat transfer coefficients. For the majority of flow regimes and in particular for vertical annular flows, RELAP5 relies on the work of Vierow and Schrock (1992) that studied the effect of noncondensable gases in a natural circulation loop. Vierow and Schrock (1992) found that the degradation in the heat transfer coefficient was a function of the gas concentration with the following correlation:

$$f_r = \begin{cases} 1 - 10X_n & \text{if } X_n < 0.063 \\ 1 - 0.938X_n^{0.13} & \text{if } 0.063 \leqslant X_n \leqslant 0.60 \\ 1 - X_n^{0.22} & \text{if } X_n > 0.60 \end{cases} \quad (1)$$

where $f_r$ is the degradation factor in heat transfer and $X_n$ is the non-condensable gas concentration. Nagae et al. (2007) and Park et al. (2003) pointed out the limitations of system codes in predicting the heat transfer in the presence of non-condensable gases. In addition, other researchers such as Yeong-Jun et al. (2015); Kang and Yun (2019) or Lee et al. (2016b) have derived new interesting empirical correlations. Although the authors of the present work acknowledge the limitations of RELAP5 to correctly simulate the heat transfer process, it is considered that the tool is sufficiently validated to carry out this analysis. Nevertheless, RELAP5 is licensed in several countries to perform Deterministic Safety Analysis including the treatment of non-condensable gases.

## 3. The ASVAD valve

The Automatic Safety Valve for Accumulator Depressurization (ASVAD) (Laborda Rami, 2017) is a unique kind of safety valve specifically designed to avoid the nitrogen injection. The ASVAD valve has been patented by several patent offices and is certified as nuclear grade 2 (Laborda Rami, 2019; Laborda Rami, 2015). ASVAD is a very simple element. One of their main advantages is that the valve is fully passive and automatic (category A). It only actuates when the accumulator pressure drops below a preset pressure. This pressure can be adjusted to the point when the accumulator is estimated to become empty of water.

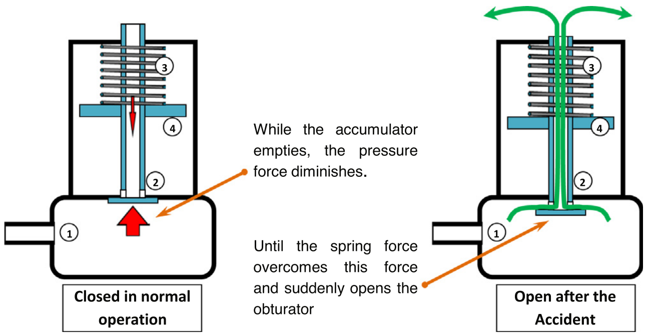


**Fig. 1.** ASVAD valve, description of the components and working principle.

Fig. 1 is a simplified representation of the ASVAD Valve and to describe the working principle. It has a pressurized chamber (1) connected to the accumulator nitrogen side. This chamber is sealed by a hollow obturator (2) and a gasket. There are a preloaded spring (3) by an adjustment disc (4) threaded over the obturator. Fig. 2 presents a detailed design drawing of the valve.

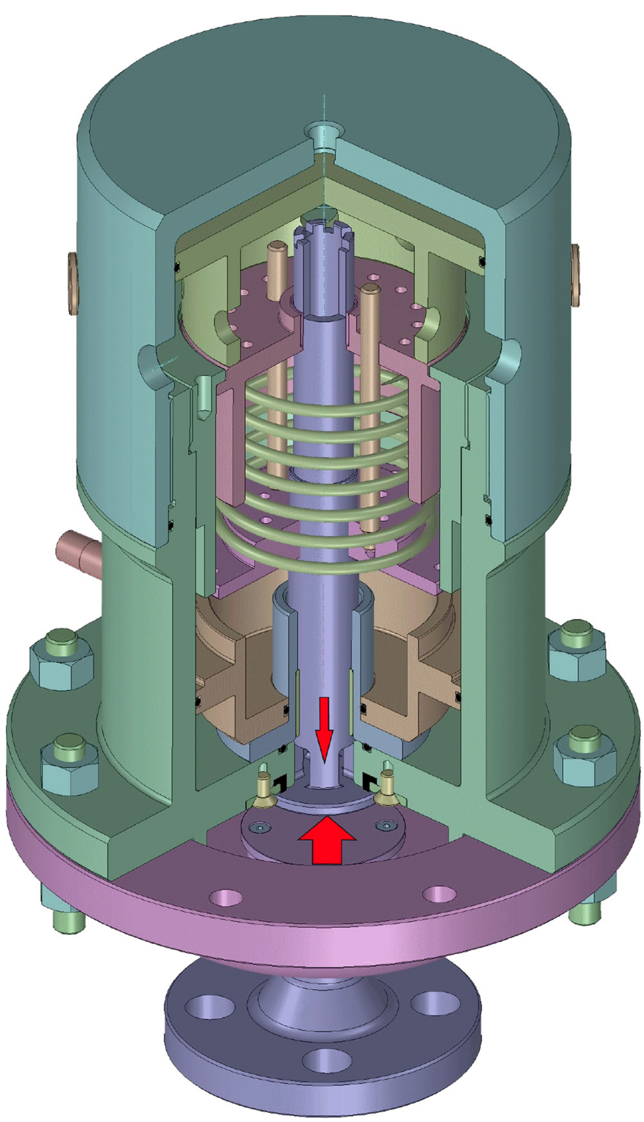

**Fig. 2.** ASVAD valve, design configuration.

The basis of the ASVAD valve operation is the imbalance between the forces exerted over the obturator. On the bottom side, there is the force exerted by the accumulator internal pressure. This force firmly pushes up the obturator keeping it closed. On the upper side, there is the force exerted by a preloaded spring. This force is constant and pushes down the obturator trying to open it. While the force exerted by the accumulator normal pressure (thick arrow) is greater than the force exerted by the spring (thin arrow), the obturator remains firmly closed. During normal operation, the pressure in the accumulator is around 4.5 MPa. The valve can only open once the pressure drops to 1.5 MPa, then the force ratio is 3:1, therefore the valve will remain permanently closed.

The spring is preset to the same force of the nitrogen pressure when the accumulator gets empty (at around 1.5 MPa). So when these circumstances are reached, the spring can overcome the force done by the residual pressure and suddenly pushes down the obturator. This opens the communication from the pressure chamber (1) across the obturator inner holes, to the outside. Once the obturator has left its seat, the pressure in the chamber will falls even more, leaving the valve permanently open due to the continuous spring action.

After its action, all the nitrogen from the accumulators is exhausted to the containment atmosphere, thus fully avoiding their injection to the RCS. This action only happens when the accumulator gets depleted from its water. Being fully passive and automatic guarantees its proper work without any operator action even during Station Blackout (SBO) scenarios.

## 4. Test 6–2: 0.1% RPV bottom small break LOCA

Test 6–2 was part of the international OECD/NEA ROSA 1 project which dealt with thermal–hydraulic safety issues in PWR reactors. The project started in 2005 and lasted for 4 years. In particular, it focused on the validation of simulation models and methods for various complex phenomena that may occur during design-basis accidents (DBA) and beyond-DBA and to increase the level of detail and accuracy in the analyses of the key phenomena during transients and accidents of interest. The project consisted on an experimental program at the LSTF facility.

The LSTF test facility, located in Tokai-Mura (Japan), has been extensively used to investigate the integral behaviour of PWR reactors under accidental conditions (The ROSA-V Group, 2003). The facility replicates the entire primary system and most of the secondary system of the Tsuruga unit 2 nuclear power plant (NPP), a 4-loop Westinghouse design. The facility was designed following the power to volume scaling principle (Navahandi et al., 1979) with a scaling k-factor of 1:48. The 4-loops where lumped in two loops, thus achieving a scaling ratio of 1:24 in the loops. The fuel rods are simulated by means of electrical heater rods with different relative powers to simulate the different rates of burned fuel. The dimensions of the rods are the same as the 17x17 fuel assembly of the reference PWR.

Test 6–2 was started by opening the 0.1% break in the lower plenum (LP). The break was modeled by using a 3.2 mm inner-diameter sharp edge orifice mounted downstream of a horizontal pipe connected to the LP. The scram signal was set to be dependent on the primary pressure by a set-point of 12.97 MPa initiating the core power decay, the primary coolant pumps coastdown, the termination of the feedwater system and the closure of the main steam isolation valve Takeda et al., 2006. The control logic of Test 6–2 is detailed in Table 1.

The safety signal (SI) signal was generated when the primary pressure decreased below 12.27 MPa and it was ensued by initiation of the auxiliary feedwater (AFW). Thirty minutes after the gen-

**Table 1**
Control logic of Test 6–2 (Takeda et al., 2006).

| Event | condition |
|---|---|
| Break | Time zero |
| Generation of scram signal | Primary pressure = 12.97 MPa. |
| PZR heater off | Generation of scram signal or PZR liquid level below 2.3 m |
| Initiation of core power decay curve simulation | Generation of scram signal |
| Initiation of primary coolant pump coastdown | |
| Turbine trip (closure of stop valve) | |
| Closure of main steam isolation valve | |
| Termination of main feedwater | |
| Generation of SI signal | Primary pressure = 12.27 MPa |
| Opening and closing of the SG relief valves | SG secondary-side pressure = 8.03/7.82 MPa |
| Initiation of auxiliary feedwater | Generation of SI signal |
| Initiation of asymmetrical SG secondary-side depressurization as AM action to achieve a depressurization rate of 55 K/h in the primary system | 30 min after generation of SI signal |
| Initiation of accumulator system | Primary pressure = 4.51 MPa |
| Initiation of low pressure injection system | RPV lower plenum pressure = 1.24 MPa |

eration of the SI signal, asymmetrical steam generator secondary-side depressurization as accident management action was activated in order to achieve a depressurization rate of 55 K/h in the primary system. This is the depressurization rate of Westinghouse designs. The accumulators started to discharge when the primary pressure was reduced below 4.51 MPa, while the injection of the LPSI system started when the lower plenum pressure fell below 1.24 MPa. The HPSI was disabled for this test. The pressure set-points for the opening and closure of the SG relief valves are 8.03 and 7.82 MPa respectively.

In order to protect the electrically heated rods that simulate the core, the maximum temperature of the cladding is monitored and set-points trigger a power reduction. For temperatures above 958 K, the core power is reduced with different stepwise reductions. If the temperature reaches 973 K the core power is completely shutdown.

Further details on the experimental procedures and results can be found in Ref. Takeda et al. (2006).

## 5. Results

### 5.1. RELAP5 model

All calculations in the present analysis have been performed with the RELAP5 system code developed by the US nuclear regulatory commission (NRC). The ANT group at UPC has developed and maintained a RELAP5 nodalization of the LSTF facility for the last 15 years. The nodalization has been used to simulate a total of 11 experiments which has allowed the validation and assessment of the capabilities of RELAP5 for thermal hydraulics phenomenology. Some examples of such applications were presented by Martinez-Quiroga et al. (2012, 2018) and Freixa et al. (2015).

The full model nodalization used in the present work is shown in Fig. 3. The core region is simulated by 13 parallel channels with 20 axial nodes. The 13 channels correspond to fuel assemblies or groups of fuel assemblies having the same power. Cartesian cross-flows were used to distribute them radially. In LSTF there are 8 control rod guide tubes and these were here modelled with 8 distinct pipes connected to the corresponding channel at the bottom and all connected to the same volume that represents the Upper Head (UH). The U-tube bundles are modelled with 5 pipe components to account for the difference in height.

### 5.2. Post-test calculation

Table 2 shows the chronology of the main events that occurred in Test 6–2 comparing the experimental values with the calculated ones. The simulation was able to reproduce correctly the timing of the events. All events took place with a difference of less than 10%. It has to be considered that this experiment is rather long and the capacity of a system code to predict the evolution decreases as the transient evolve. Differences in the timing of the events of the order of thousands of seconds can be expected for such a long transient simulation (Freixa et al., 2020).

The most relevant results of Test 6–2 are shown in Fig. 4 where the simulation results are compared with the experiment. The figure displays the cladding temperature, the primary and secondary pressures, the loop mass flow-rates and the RPV collapsed water levels. Overall, a good agreement between simulation and experimental results was obtained. In the following paragraphs a detailed description is provided on the overall evolution of the transient, while further details on the effects of the nitrogen into the system are provided in the following subsection.

The primary and secondary pressures are shown in the top graph of Fig. 4. Once the depressurization is started in loop B, the primary pressure remains close to the loop A secondary pressure until the reflux-condenser mode in this loop is interrupted (around 4000 s). In the calculation, the primary pressure is partly dragged down by the secondary side depressurization of loop B. Afterwards the primary pressure in both the experiment and the simulation follows the loop B depressurization.

The nitrogen injection starts around 10000 s, and the loop B mass flow is quickly and clearly affected. The primary pressure also rises momentarily due to nitrogen expansion. The intermittent flow is due to the oscillating pressure increase due to the gas heating and expansion during the gas inflow.

As shown in Fig. 4, the primary pressure stabilizes around 1.6 *MPa* during the latter period of the test (12000–25000 s). The nitrogen concentrates in the U-tubes and induces a degradation of the heat transfer from the primary to the secondary system. In order to keep a balanced heat extraction, the delta T between the primary and secondary system increases, thus the primary system stabilizes at a higher value than expected. And as a consequence, the set-point for the LPSI intervention is only reached after the core has been uncovered. Temperatures in the core increase until the core protection is triggered, core power is stepwise reduced for temperatures above 950 K. Due to the stepwise core power reduction, the experimental and simulation powers are reduced at different values. The experimental power is reduced by 85% and the simulation power by 65%.

The evolution of the natural circulation in both loops is well predicted (middle graph of Fig. 4). After the primary pumps are completely stopped, the computed mass flows drop to the correct value. Afterwards, the natural circulation is slightly overestimated by the calculation and as a consequence the primary pressure depressurizes further as more heat is being extracted (time between 2500 and 4000 s). The end of natural circulation in loop A occurs at around 2500 s similarly as in the experiment.

The maximum cladding temperature was measured in position 7 on rod(4,4) of element B17 (top graph of Fig. 4). Two peaks where observed in the experiment, the first one was quenched by a temporary injection of the LPSI system, while the second peak reached the core protection set point, triggering a reduction of the core power. The phenomenology taking place here is as follows:

- The pressure cannot be reduced to the LPSI setpoint, so mass inventory is continuously diminishing.

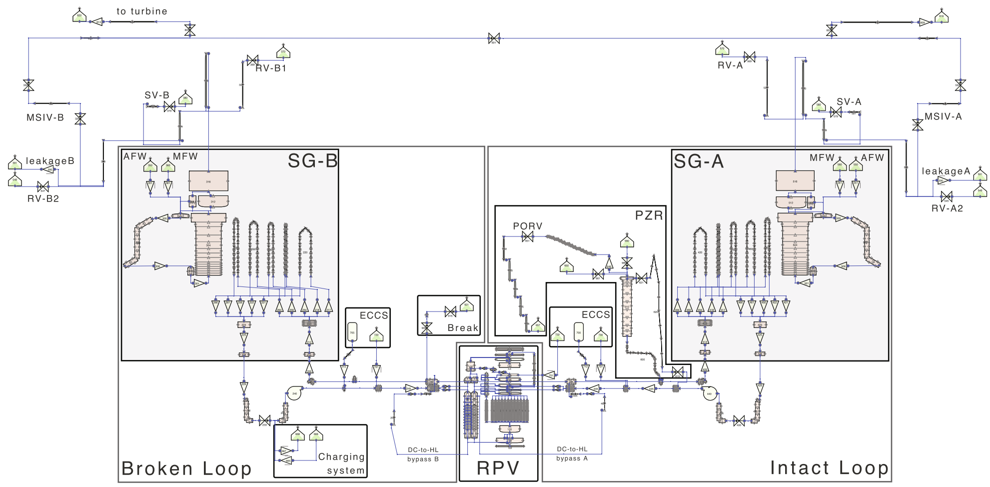


**Fig. 3.** RELAP5 nodalization of the LSTF facility.

**Table 2**
Chronology of the main events in Test 6–2 (Takeda et al., 2006).

| Event | Experimental | RELAP5 | Err |
|---|---|---|---|
| | data (s) | calculation (s) | (%) |
| Break valve opened | 0 | 0 | |
| Scram signal (primary pressure = 12.97 MPa) | 569 | 582 | 2.3 |
| SI signal (primary pressure = 12.27 MPa) | 736 | 681 | −7.5 |
| Primary coolant pumps stopped | 819 | 843 | 2.9 |
| Asymmetrical SG secondary-side depressurization (30 min after SI signal generation) | 2548 | 2481 | −2.6 |
| Closure of SG RV in loop with PZR | 2679 | 2474 | −7.7 |
| Initiation of accumulator system (pressure = 4.51 MPa) | About 5150 | 5120 | −0.6 |
| Inflow of nitrogen gas from accumulator tank into loop with PZR | About 10030 | 10028 | 0.0 |
| Inflow of nitrogen gas from accumulator tank into loop without PZR | About 11070 | 11736 | 6.0 |
| Temporary increase in primary pressure appeared twice | 12000 | 12000 | 0.0 |
| Core uncovery | About 20400 | 20870 | 2.3 |
| Actuation of LPSI system (RPV lower plenum pressure = 1.24 MPa) | About 21940 | 21630 | −1.4 |
| Core power decrease by LSTF core protection system (Max. fuel rod surface temperature = 970 K) | About 23270 | 23510 | 1.0 |
| Second actuation of LPSI system (RPV lower plenum pressure = 1.24 MPa) | About 23320 | 22700 | −2.7 |
| Break valve closed, end of transient | 24034 | 25000 | 4.0 |

- When core uncovery starts, the amount of steam generated in the core is reduced, decay heat energy is invested in increasing cladding temperatures in the core. This means that the primary pressure decreases and the LPSI signal can be finally reached.
- LPSI cold water enters the core causing either partial or total quenching and at the same time generating a large amount of steam. Therefore, primary pressure increases and LPSI may cease.
- Without LPSI, the core level decreases again and the cycle is repeated.

In the experiment, the core was fully quenched in the first cycle and for the second cycle the core protection signal was reached and power was reduced. In the calculation, one can observe a similar behaviour, although in this case the LPSI only replenishes the core partially and the PCT keeps increasing until we reach the core protection. Later on, the process is repeated several times and the LPSI system does not manage to bring the plant to a safe shutdown condition. Since the core power has been reduced the calculation can be stopped.

The core and upper plenum levels are displayed in the bottom graph of Fig. 4. The overall behaviour as simulated by the UPC RELAP nodalization is in accordance with the experiment. There is a time delay on the plunging of the core level at 20000 s. Later, the start of the LPSI also takes place with some time differences.

### 5.3. Phenomenology related to non-condensables

Fig. 5 displays the results related to the inflow of the nitrogen into the primary system. The top graph shows the pressure evolution in the primary system and the SG B. The graph in the middle shows the mass flow evolution in Loop B. In the bottom plot, the Acc levels along with the total amount of nitrogen inflow into the primary system are shown.

The amount of nitrogen injected is under predicted by RELAP for some part of the transient but later the total mass of injected nitrogen is correctly predicted. However, one has to bear in mind that the experimental injected nitrogen was inferred from the pressure and temperature conditions in the Accumulator and by applying ideal gas laws, the uncertainty of the measurement was not provided in the experimental report but is deemed to be high.

#### 5.3.1. Intermittent interruption of natural circulation

At around 10000 s, nitrogen starts to flow into the primary system. At this moment, Loop B presents two-phase natural circulation and the nitrogen is quickly dragged through the circuit. Heat transfer in the U-tubes is reduced and the primary pressure reduction is greatly diminished. During two-phase natural circulation, condensation is taking place in the U-tubes increasing locally the nitrogen concentration. Slugs of nitrogen are formed which reduce heat transfer even further. Whats more, natural circulation even halts due to the presence of nitrogen. When the circulation stops, primary pressure increases and so does the difference of saturation temperatures between the primary and the secondary. This means that the driving force for circulation is regained. This process of interruption and restart of natural circulation happens twice in the experiment while in the calculation it takes place 6 times. The primary side water inventory is being reduced until reflux and condensation conditions are attained (at around 13000 s).

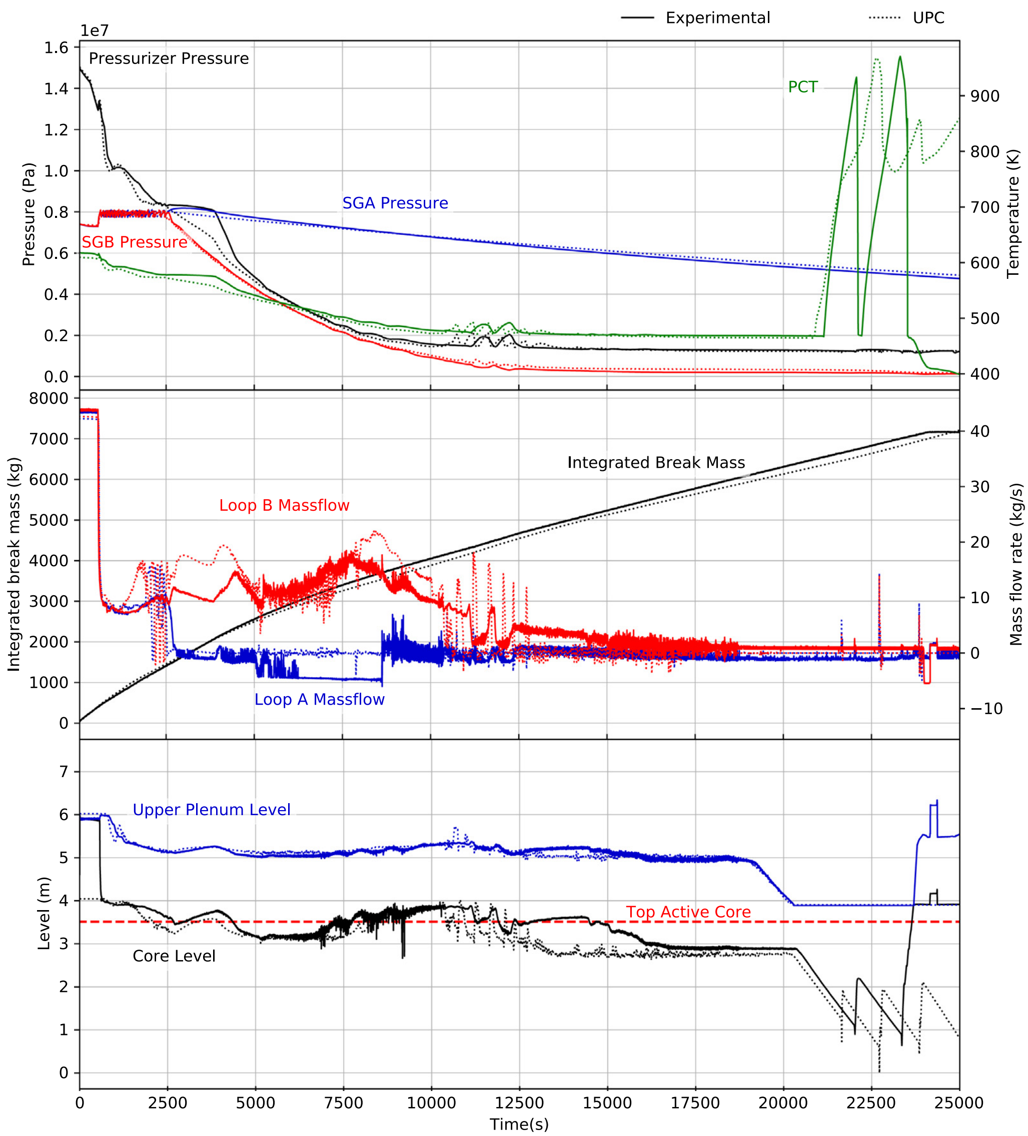


**Fig. 4.** RELAP results for Test 6–2. Top - Cladding temperature (green line), Pressurizer pressure (black line) and SG pressures of Loop A (blue line) and Loop B (red line).Middle - Mass flow in Loop A (blue line) and Loop B (red line), integrated break mass (black line)Bottom - Upper plenum (blue line) and Core level (black line), top of active core (red line).

For the experimental data, the middle graph in Fig. 5 seems to show sustained natural circulation until the end of the experiment. However, the level in the U-tubes dropped at around 13000 s and they remained empty for the rest of the experiment indicating that natural circulation ended at this point and that the flow measurement from this point is not reliable.

### *5.3.2. Deterioration of heat transfer during reflux and condensation conditions*

Once the reflux-condensation are established, the pressure of the primary system will be governed by the heat transfer to the secondary side. The RELAP code adjusts the heat transfer coefficient in the presence of non-condensables by adding a correction to the correlation in place. This adjust meets the Vierow & Schrock correlation described in Section 2. As can be seen in Fig. 5 the primary pressure in the calculation agrees well with the experiment.

Another relevant point is that, shortly after the nitrogen entry, its effects on the primary pressure become evident. Just 50 mol is enough in order to diminish -and maintain- the primary flow near to zero. The flow drop combined with the heat transfer degradation nearly stops the SG heat transfer during the whole experiment strongly diminishing their capacity to extract heat.

### *5.4. Case without core protection*

The core power in Test 6–2 had to be reduced to protect the electrically heated rods in the core. Once the core power is reduced the experimental data is no longer representative of the studied scenario. It is worth remembering that the control logic of the experiment reduces the core power if cladding temperatures exceed 958 K, and that the reduction is carried out stepwise until 973 K threshold when the power is fully shutdown. Since the post-test calculation has shown to be accurate enough to represent the phenomenology in the experiment, it is possible now to estimate with a calculation a possible outcome of the experiment considering that the core power is not reduced. Fig. 6 displays the results of the post-test calculation without the core protection system. Three cases are shown:

1. the experiment where the core power is reduced by 87%,

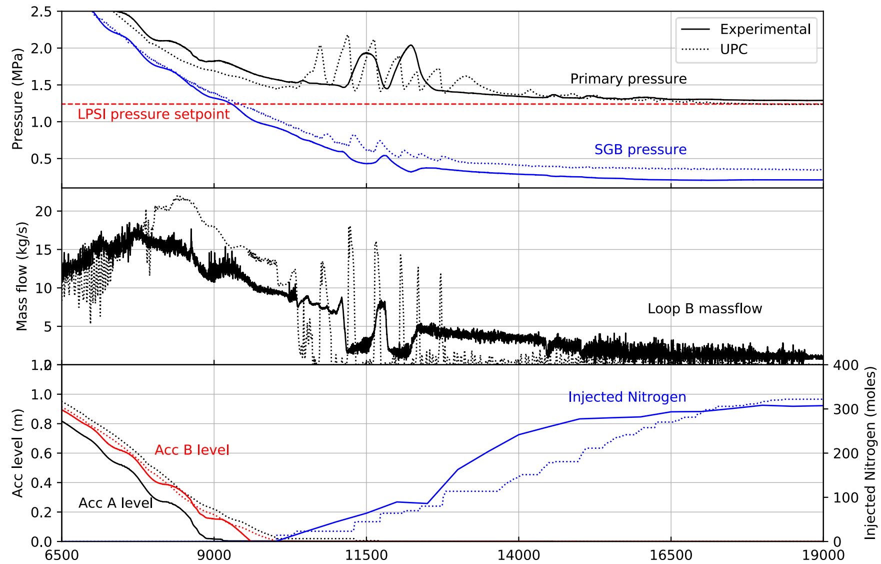


**Fig. 5.** Post test results in relation to the nitrogen inflow. Top: Primary and secondary (SG B) pressure evolution. Middle: Loop B mass flow evolution. Bottom: Acc levels and total injected nitrogen into the primary system. Time frame 6500 to 19000 s.

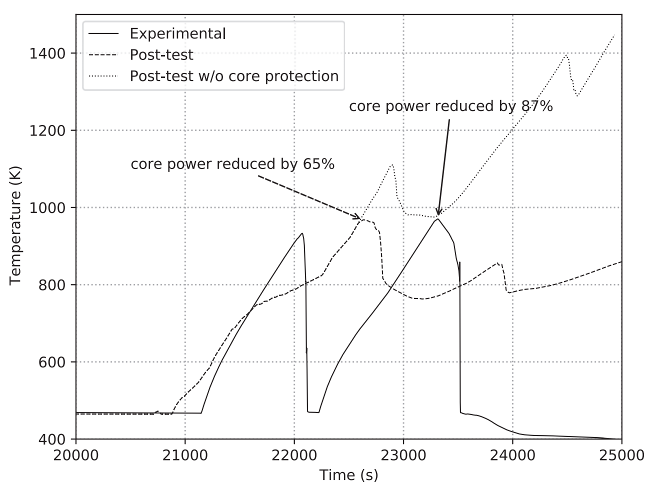


**Fig. 6.** Maximum cladding temperature results for Test 6–2 compared to the post-test and the post-test without core protection.

2. the post-test calculation with a power reduction of 65%,
3. the post-test calculation with no power reduction.

We can see that in this case the PCT keeps increasing until we reach temperatures close to the acceptance criteria limit of 1473 K. The simulation failed at a temperature of 1430 K. This result indicates that probably, the experiment would reach core damage if core protection would not be applied. Nevertheless, it is important to keep in mind that the entrance of the LPIS during the first PCT increase quenched the core in the experiment and the calculation did not show a full quenching.

### *5.5. Performance of the ASVAD valve in the scenario*

After the evaluation of the post-test calculation of the scenario, it is possible to test the effects of implementing the ASVAD valve in the scenario. The ASVAD valve is modeled in RELAP5 with a simple valve and a control logic. The valve will open when the predefined setpoint is reached. The effect in the boundary conditions is straight forward, once the valve is open the pressure in the accumulator is lower than the primary pressure and the accumulator check valve closes terminating the accumulator injection.

Fig. 7 shows the results for different pressure set-points for the ASVAD valve (1.3, 1.4, 1.5 and 1.6 MPa). The figure shows the primary pressure, the Acc levels, the core level and the PCT. All calculations present the same results up to the actuation of the ASVAD valve at around 9000 to 10000 s. The differences can be seen in the water level of the Acc and its implications on the evolution of the primary pressure.

Setting the ASVAD opening setpoint over 1.5 MPa, avoids the effects of the nitrogen and prevents its complications even though some water from the accumulators will not be injected. For the present case, all set-points above 1.5 MPa will allow the effective depressurization and reaching —and maintaining —the LPSI set-point about 10000s earlier than in the experiment. Around 1.5 MPa is the adequate setpoint which the nitrogen injection is avoided and the accumulator water is fully injected.

When setting the set-point at 1.4 and 1.3 MPa, some nitrogen is injected and its adverse effects can be clearly observed. Firstly, as soon as some nitrogen enters the primary system natural circulation interruption and restart takes place several times. Afterwards, the pressure is reduced until the LPSI system is activated. The injection of cold water pushes all the nitrogen to the U-tubes reducing drastically heat transfer so pressure increases. Without LPSI, the nitrogen concentration in the U-tubes decreases again and pressure is reduced until reaching the LPSI setpoint. This process may repeat several times but in the long term, the cooling of the core is guaranteed.

Setting the setpoint below 1.24 MPa would not provide any additional information since the LPSI system starts at 1.24 MPa and it sustains the primary pressure by the injection of substantial amount of coolant so the ASVAD valve set-point would not be reached.

#### *5.5.1. ASVAD valve and no active injection*

The effect of the ASVAD valve allows for a quick actuation of the LPSI system for all the pressure set-points that are above the LPSI setpoint. However, the ASVAD valve benefits are not only related with the actuation of the LPSI. The fact that the reflux and condensation conditions are kept with its full effectiveness allows for a further depressurization through the actions on thermal hydraulics

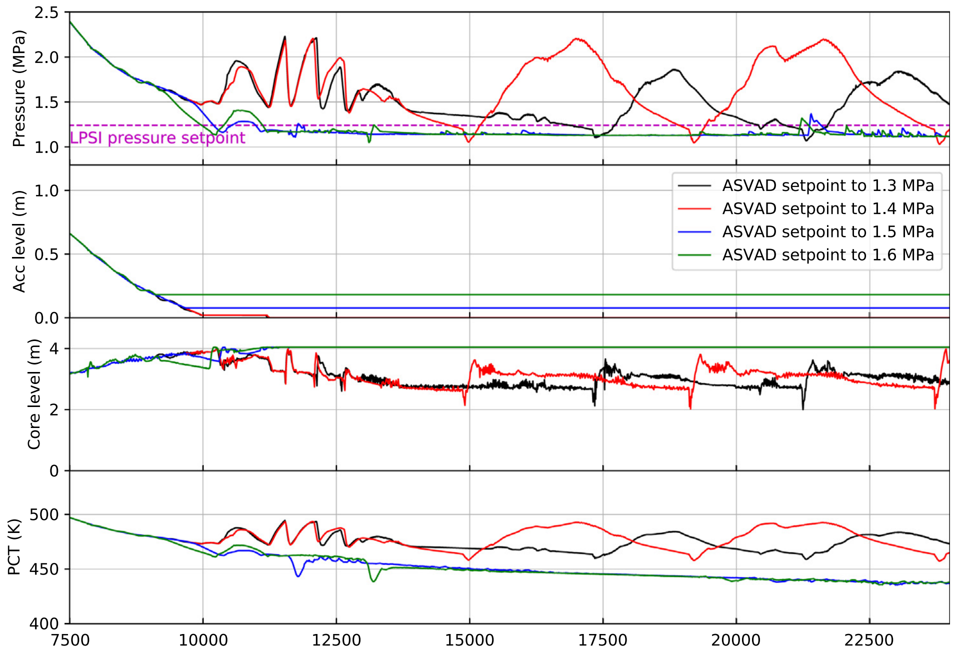


**Fig. 7.** Main results of the ASVAD performance considering different pressure set-points. From top to bottom: primary pressure, Acc level, core level and PCT.

secondary system. A lower primary pressure implies that the break flow is reduced. In this section a calculation considering the ASVAD valve (setpoint of 1.6 MPa) and the unavailability of the LPSI systems is presented. This means that no active injection is supposed in this scenario. The results of this scenario are compared with the two previous cases:

1. original scenario without core protection,
2. original scenario with the ASVAD valve (1.6 MPa),
3. original scenario with the ASVAD valve (1.6 MPa) and unavailability of the LPSI.

Fig. 8 shows the results of the cladding temperature for the three cases. In the case without core protection, the temperatures increase dangerously and the calculation crashes when we are close to the licensing limit of 1473 K. When the ASVAD valve is applied in combination with the LPSI system, the primary pressure is dragged consistently down by the secondary depressurization

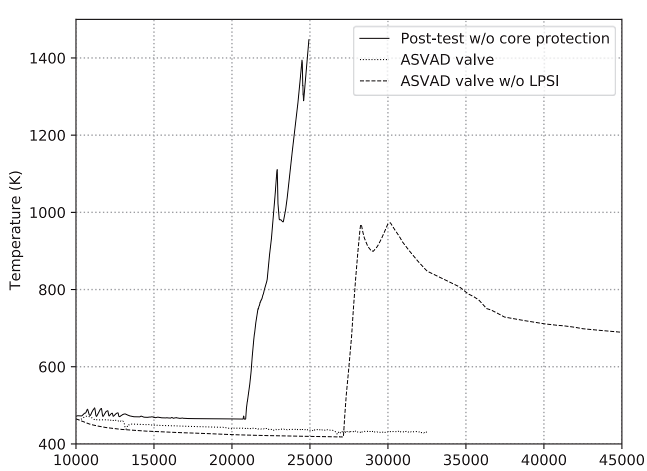


**Fig. 8.** Cladding temperatures for three cases: Post-test without core protection, post-test with ASVAD and Post-test with ASVAD and without LPSI.

and the LPSI system is able to inject water without interruption. In this case, the core coolability is guaranteed at all times and the calculation is stopped at around 33000s.

In the case where the LPSI is not available, still the ASVAD valve is quite effective in reducing the cladding temperatures. As there is no nitrogen intrusion, the heat transfer is not affected and is effective enough to cool the core. The secondary side depressurization drags down the primary pressure. Since the pressure is reduced, the break flow reduces as well and the core uncovery is significantly delayed (6000 s), at this time the core power is lower and the steam circulation is more effective in extracting heat due to the presence of moisture. Nevertheless, one needs to consider that heat losses in an ITF are proportionally more significant than in the full size NPP and, therefore, it is not possible to extrapolate this behaviour to the NPP. Further analysis of this scenario would require a scaling analysis of the heat losses and other scaling distortions. Even though the results cannot be directly extrapolated to the reactor size, this calculation shows that the benefits of the ASVAD valve are very significant.

This is just one situation where the ASVAD valve could improve the safety of the reactor and the intention of the present publication is to show the possible benefits of this system. However, a broad analysis of the performance of the system should be carried out to understand its impact in all the possible situations. As is shown in the study, one of the main advantages could be to allow the RCS pressure to decrease to lower values without compromising the heat transfer in the SGs. This could give more options to the emergency organization to reach a sustainable core cooling at lower pressures.

Future research should be focused on finding the possible drawbacks (if any) when using the ASVAD valve in the accumulators of a PWR.

## 6. Conclusions

The presence of non-condensable gases in the primary system poses different complications that jeopardize the safety of a PWR reactor. Nitrogen may be injected through the accumulator system if this is not correctly isolated after the full discharge of the subcooled water. Research on this issue has been carried out by the international community by means of both experimental programs and the improvement of computational methods. Current system codes are capable of reproducing the transport of non-condensable gases in two-phase flow environments.

Test 6–2 from the LSTF facility is one of the relevant experiments where the adverse effects of the nitrogen injection from the accumulators are clearly observed. The experiment results show that a relatively small quantity of nitrogen can significantly disturb the cooling through the SGs. In the present work, Test 6–2 has been simulated with the RELAP5 system code. The results of the post-test calculation are in close agreement with the experiment which has allowed to investigate additional the postulated scenarios.

Firstly, a calculation without the core protection has been carried out that shows that the scenario could lead to core damage. Afterwards, the scenario has been simulated with the ASVAD valve and several different pressure set-points. The results show that the ASVAD valve would be effective to avoid the nitrogen intrusion with a pressure setpoint above 1.5 MPa. Nevertheless, with a slightly lower pressure set-points the core remains covered at all times.

Finally, a calculation simulating an SBO scenario without any active safety injection (including the LPSI) has been carried out. Even in this case, the ASVAD valve helps to reduce the primary pressure so that the break flow is reduced and the core uncovery is reached about 6000 s later. At this point the power has been reduced and the increase in cladding temperatures is below 1000 K. The ASVAD valve has proven to be very effective to avoid core damage with the present scenarios. Future research will focus on the testing of the ASVAD performance in a broad spectrum of scenarios with a full size NPP model.

## CRediT authorship contribution statement

**Jordi Freixa:** Conceptualization, Methodology, Formal analysis, Software, Investigation, Visualization, Writing - original draft. **Arnaldo Laborda:** Writing - original draft, Writing - review & editing. **Victor Martinez-Quiroga:** Validation, Investigation, Software, Formal analysis.

## Declaration of Competing Interest

The authors declare that they have no known competing financial interests or personal relationships that could have appeared to influence the work reported in this paper.

## Acknowledgements

The present work contains findings that were produced within the OECD/NEA ROSA-1. The authors are grateful to the Management Board of the project for their consent to this publication. The authors also want to thank the Spanish Safety Council (CSN) that has partly financed the participation of UPC to the project.

## References

Austregesilo, H., Bals, C., Hora, A., Lerchl, G., Romstedt, P., 2003. Mod 2. 0 Cycle A Models and Methods. Tech. Rep. November.

D'Auria, F., Aksan, N., Bestion, D., Galassi, G.M., Glaeser, H., Hassan, Y.A., Jeong, J.J., Kirillov, P.L., Morel, C., Ninokata, H., Reventós, F., Rohatgi, U.S., Schultz, R.R., Umminger, K., 2017. Thermal Hydraulics in Water-Cooled Nuclear Reactors. Woodhead Publishing Series in Energy..

DeVuono, A.C., Christensen, R.N., 1984. Experimental investigation of the pressure effect on film condensation of steam-air mixture at pressure above atmospheric. Fundamentals of Phase Change: Boiling and Condensation 38, 73–80.

Freixa, J., 2012. Remarks on Consistent Development of Plant Nodalizations: An Example of Application to the ROSA Integral Test Facility. Tech. Rep. TM—12, Paul Scherrer Institut..

Freixa, J., Martínez-Quiroga, V., Zerkak, O., Reventós, F., 2015. Modelling guidelines for core exit temperature simulations with system codes. Nuclear Engineering and Design 286, 116–129. URL http://linkinghub.elsevier.com/retrieve/pii/S0029549315000850.

Freixa, J., Martinez-Quiroga, V., Reventós, F., 2020. Modelling guidelines for safety analysis of Station Black Out sequences based on experiments at the PKL test facility. Annals of Nuclear Energy 138,. https://www.sciencedirect.com/science/article/pii/S0306454919306899?dgcid=author 107179.

Gallardo, S., Abella, V., Verdú, G., 2011. Assessment of TRACE 5.0 against ROSA Test 6–2, Vessel Lower Plenum SBLOCA. Tech. Rep. February.

IAEA, 2009. Passive Safety Systems and Natural Circulation in Water Cooled Nuclear Power Plants. Tech. rep., IAEA. https://www-pub.iaea.org/MTCD/Publications/PDF/te_1624_web.pdf.

Information Systems Laboratories, 2010. RELAP3.3 MOD3.3 Code Manual VOLUME IV: Models and Correlations. Tech. Rep. NUREG/CR-5535/Rev P4-Vol IV, Information Systems Laboratories, Rockville, Maryland..

Kang, J., Yun, B., 2019. An experimental study of steam condensation with the presence of air under free convection condition. In: Nureth-18. pp. 1893–1906..

Laborda Rami, A., 2015. Passive Depressurisation System For Pressurised Receptacles. URL https://patentscope.wipo.int/search/en/detail.jsf?docId=WO2015169975.

Laborda Rami, A., 2017. The nitrogen injection threat in PWR reactors: Weakness of current strategies and ASVAD, the new passive solution. In: CN-251 Topical Issues in Nuclear Installation Safety (IAEA). URL https://nucleus-qa.iaea.org/sites/gsan/act/cn-251/papers/56-IAEA_Asvad_abstract_rev_1.pdf.

Laborda Rami, A., 2019. Passive depressurization system for pressurized containers. URL https://uspto.report/patent/grant/10,366,796.

Lee, K.-W., No, H.C., Chu, I.-C., Moon, Y.M., Chun, M.-H., 2006a. Local heat transfer during reflux condensation mode in a U-tube with and without noncondensible gases. International Journal of Heat and Mass Transfer 49 (11–12), 1813–1819. http://linkinghub.elsevier.com/retrieve/pii/S0017931005006848.

Lee, J., Park, G.-C., Cho, H.K., 2016b. Validation of wall film condensation model in the presence of NC gas for two-fluid model. In: NUTHOS-11, pp. 1–15.

Liu, T.-J., 2001. Reflux condensation behavior in a U-tube steam generator with or without noncondensables. Nuclear Engineering and Design 204 (1–3), 221–232. http://linkinghub.elsevier.com/retrieve/pii/S0029549300003137.

Martinez-Quiroga, V., Reventós, F., Pretel, C., 2012. Post-Test Calculation of the ROSA/LSTF Test 3–2 Using RELAP5/Mod3.3. NUREG/IA NUREG/IA-0. http://pbadupws.nrc.gov/docs/ML1208/ML12083A012.pdf..

Martinez-Quiroga, V., Freixa, J., Reventos, F., 2018. PVST, a tool to assess the Power to Volume scaling distortions associated to code simulations. Nuclear Engineering and Design 332 (March), 173–185. https://doi.org/10.1016/j.nucengdes.2018.03.035.

Mukin, R., Clifford, I., Zerkak, O., Ferroukhi, H., 2018. Modeling and analysis of selected organization for economic cooperation and development PKL-3 station blackout experiments using TRACE. Nuclear Engineering and Technology 50 (3), 356–367. https://doi.org/10.1016/j.net.2017.12.005.

Nagae, T., Chikusa, T., Murase, M., Minami, N., 2007. Analysis of noncondensable gas recirculation flow in steam generator U-Tubes during reflux condensation using RELAP5. Journal of Nuclear Science and Technology 44 (11), 1395–1406.

Navahandi, A.N., Castellana, S., Moradkhaniav, E.N., 1979. Scaling laws for modeling nuclear reactor systems. Nuclear Science and Engineering 72.

NEA, 2013. Final Integration Report of the OECD/ NEA ROSA Project. Tech. rep., Nuclear Energy Agency.

Noel, B., Derauz, R., 1994. Reflux condenser mode with non-condensabel Gas: assessment of CATHARE against BETHSY Test 7.2C. Nuclear Engineering and Design 149.

OECD/NEA, 2017. Final Integration Report of the Rig-of-Safety Assessment (ROSA-2) Project. Tech. rep. URL www.oecd-nea.org..

Park, H.-S., No, H.C., Bang, Y.S., 2003. Analysis of experiments for in-tube steam condensation in the presence of noncondensable gases at a low pressure using the RELAP5/MOD3.2 code modified with a non-iterative condensation model. Nuclear Engineering and Design 225 (2–3), 173–190. http://linkinghub.elsevier.com/retrieve/pii/S0029549303001766..

Riikonen, V., Kouhia, V., Kauppinen, O., Sjovall, H., Hyvarinen, J., 2018. Experimental observation of adverse and beneficial effects of nitrogen on reactor core cooling..

Song, C.-H., Choi, K.-Y., Kang, K.-H., 2015. ATLAS program for advanced thermal-hydraulic safety research. Nuclear Engineering and Design 294, 242–261. https://www.sciencedirect.com/science/article/pii/S0029549315003982.

Steinbrück, M., Oliveira da Silva, F., Grosse, M., 2017. Oxidation of Zircaloy-4 in steam-nitrogen mixtures at 600–1200 C. Journal of Nuclear Materials 490, 226–237.

Takeda, T., Suzuki, M., Asaka, H., Nakamura, H., 2006. Quick-look Data Report of OECD/NEA ROSA Project Test 6-2 (0.1% Pressure Vessel Bottom Small Break LOCA Experiment). Tech. Rep. JAEA-Research 2006-9002, Japan Atomic Energy Agency..

Takeda, T., Ohnuki, A., Kanamori, D., Ohtsu, I., 2016. ROSA/LSTF Tests and RELAP5 Posttest analyses for PWR safety system using steam generator secondary-side depressurization against effects of release of nitrogen gas dissolved in accumulator water. Science and Technology of Nuclear Installations, 2016..

The ROSA-V Group, 2003. ROSA-V Large Scale test facility (LSTF) system description for the third and fourth simulated fuel assemblies. Tech. Rep. JAERI-Tech 2003-037, Japan Atomic Energy Agency..

Umminger, K., Dennhardt, L., Schollenberger, S., Schoen, B., 2012. Integral test facility PKL: Experimental PWR accident investigation. Science and Technology of Nuclear Installations 2012, 16. https://downloads.hindawi.com/journals/stni/2012/891056.pdf.

United States Nuclear Regulatory Commission, 2007. TRACE V5.0: Theory Manual Field Equations, Solution Methods, and Physical Models (V50rc3)..

US-NRC, 2008. NRC Generic Letter 2008-01: Managing Gas Accumulation in Emergency Core Cooling, Decay Heat Removal, and Containment Spray Systems. Tech. rep., USNRC. URL http://www.nrc.gov/reading-rm/doc-collections/enforcement/actions/reactors/ea97297.html.

Vierow, K., Schrock, V., 1992. Condensation in a natural circulation loop with noncondensable gas present. In: U.S. Seminar on Two-Phase Flow Dynamics. Berkeley, California, USA..

Woods, B.G., Groome, J., Collins, B., 2009. An assessment of PWR steam generator condensation at the Oregon State University APEX facility. Nuclear Engineering and Design 239 (1), 96–105. http://linkinghub.elsevier.com/retrieve/pii/S0029549308003804.

Yeong-Jun, J., Dong-Jae, C., Yeon-Gun, L., Sin, K., Dong-Wook, J., 2015. Experimental study of condensation heat transfer in the presence of noncondensable gas on the vertical tube. International Topical Meeting on Nuclear Reactor Thermal Hydraulics 2015, NURETH 2015 7, 6096–6109..